THE JOURNAL OF PHYSICAL CHEMISTRY C

Article

pubs.acs.org/JPCC

Surface Influence on the Metalation of Porphyrins at the Solid–Liquid Interface

Cynthia C. Fernández, Cecilia Spedalieri, Daniel H. Murgida, and Federico J. Williams*

Departamento de Química Inorgánica, Analítica y Química Física, Facultad de Ciencias Exactas y Naturales, INQUIMAE-CONICET, Universidad de Buenos Aires, Ciudad Universitaria, Pabellón 2, Buenos Aires C1428EHA, Argentina

S Supporting Information

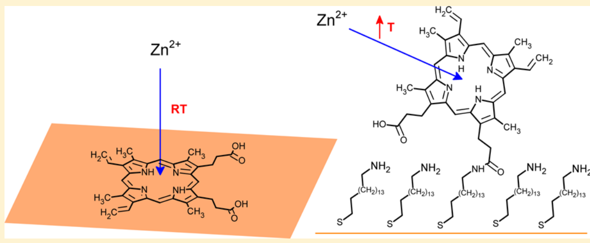

ABSTRACT: The insertion of a metal atom in the central cavity of adsorbed porphyrins is an important subject as it allows specific control over the functionality of the molecule. In this work, metalation of protoporphyrin IX (PPIX) molecules bonded directly to a Au(111) surface or to a self-assembled monolayer (SAM) on Au(111) was studied at the solid–liquid interface. X-ray photoelectron spectroscopy (XPS) and scannning tunneling microscopy demonstrate that the molecules bind to the SAM without forming aggregates and with a surface coverage below the monolayer. Near-edge X-ray absorption fine structure spectroscopy and surface-enhanced resonance Raman spectroscopy demonstrate that the molecules are bonded to the SAM with a tilted molecular plane. XPS measurements show that PPIX molecules bonded to the SAM and exposed to Zn^{2+} containing aqueous solutions are metalated to a small extent at room temperature and fully metalated at 350 K. In contrast, PPIX molecules adsorbed directly to the Au(111) surface are fully metalated at room temperature. These results show that surface–molecule interactions could have an impact on the metalation of porphyrin molecules.

■ INTRODUCTION

Porphyrin molecules are important functional building blocks that play a key role in many processes of biological importance including oxygen transport, metabolic catalytic conversion, light harvesting, and photosynthesis.[1] The chemical, optical, electronic, and magnetic properties of the molecules are modulated by the choice of the metal center giving rise to their diverse properties. Thus, porphyrins have potential applications in molecular devices including solar cells, organic light emitting devices, sensors, catalysts, and molecular electronic devices.[2−9] Derivatized porphyrins are also versatile building blocks for the creation of many different types of assemblies, including surface supramolecular structures and molecular motors.[10] Thus, studying the interaction of porphyrins with surfaces is of pivotal importance from both the applied as well as the fundamental points of view.[11,12]

Metalation of the macrocycle with metal atoms is an important reaction as it defines the properties of the molecule. This reaction involves the exchange of two aminic hydrogen atoms from the molecule central cavity with a metal atom. Although the metalation of free base porphyrin adsorbed on surfaces has been known for many years,[13] it was observed only recently at a molecular level under controlled conditions.[14] Since, there has been a great research effort to understand comprehensively the factors that control the metalation of surface porphyrins.[15] The phenomenon was observed in a variety of conditions where free base porphyrins are metalated by codeposited surface adatoms,[16] substrate metal atoms,[17] oxide lattice ions,[18] and ions from liquid solutions.[19] Very recently, the exchange of Zn^{2+} metal centers with Cu^{2+} ions from aqueous solutions was observed for surface porphyrins.[20]

In this work, protoporphyrin IX molecules (PPIX) are attached to a self-assembled monolayer (SAM) of 16-amino 1-hexadecanethiol grown on a Au(111) surface via the formation of an amide bond. The chemical reaction was monitored using X-ray and UV photoelectron spectroscopy (XPS, UPS), scanning tunneling microscopy (STM), near-edge X-ray absorption fine structure spectroscopy (NEXAFS), and surface enhanced resonance Raman spectroscopy (SERR). It is found that porphyrin molecules bind to the surface without forming aggregates and with a tilted molecular plane. This well-defined molecular system was immersed in Zn^{2+} aqueous solutions in order to study porphyrin metalation with metal ions at the solid/liquid interface.

■ EXPERIMENTAL SECTION

Materials. Photoelectron spectroscopies, near-edge X-ray absorption fine structure spectroscopy, and STM measurements were carried out using a Au(111) single crystal (MaTecK GmbH). The crystal was Ar^+ sputtered and annealed until no impurities are detected by XPS. Substrates for STM measurements were cleaned by annealing for 5 min in a hydrogen flame until the film color turned to a dark red. Protoporphyrin IX (PPIX), 16-amino-1-hexadecanethiol hydrochloride, 1-ethyl-3-(3-dimethylamino-propyl) carbodiimide (EDC), *N*-hydroxy-

Received: May 23, 2017
Revised: September 16, 2017
Published: September 18, 2017

Scheme 1. Covalent Attachment of the Protoporphyrin IX Molecules to the Amine Terminated Hexadecanethiol SAM on Au(111)

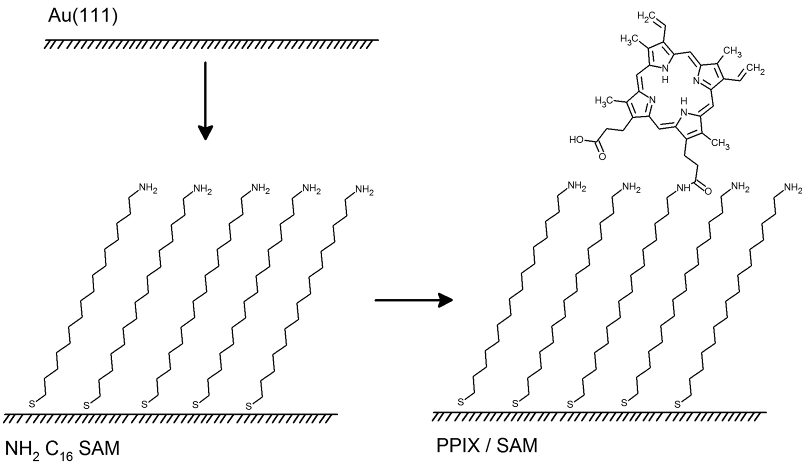

succinimide (NHS), zinc acetate, and dimethyl sulfoxide (DMSO) were obtained from Sigma-Aldrich and used as received. Absolute ethanol of analytical grade and 18 MΩ cm Milli-Q water were used to prepare solutions.

Sample Preparation. Self-assembled monolayer formation was performed under an ultrapure Ar atmosphere in a ultra-high-vacuum (UHV) chamber equipped with a transfer system that allows transferring the sample between UHV and the atmospheric liquid reactor (described fully elsewhere).[21] The clean Au crystal was placed in contact with a 1 mM solution of 16-amino-1-hexadecanethiol in ethanol at room temperature for 4 h. Meanwhile, a 0.3 mM PPIX solution in DMSO:water is incubated for 1 h in EDC (8 mM) and NHS (4 mM). After this first activation step, the SAM functionalized surface is dipped overnight in the PPIX solution. Under these reaction conditions, at least one of the PPIX carboxylic groups is expected to react with the terminal amine group exposed on the surface forming an amide bond. Multilayers of PPIX were directly deposited over the Au(111) surface to obtain reference XPS and NEXAFS spectra after evaporation of a PPIX solution that was previously placed in contact with the surface substrate. Attemps to deposit PPIX molecules over the Au(111) surface via thermal evaporation resulted in molecular fragments as observed by XPS. Thus, monolayers of PPIX molecules adsorbed directly over the Au(111) surface were prepared by immersion of the cystal in a PPIX saturated DMSO solution, followed by extensive rinsing and drying in Ar.

Photoelectron Spectroscopies. XPS measurements were performed using a UHV chamber (base pressure < $5 \cdot 10^{-10}$ mbar) with a SPECS spectrometer system equipped with a 150 mm mean radius hemispherical electron energy analyzer and a nine channeltron detector. XP spectra were acquired on grounded conducting substrates at a constant pass energy of 20 eV using a monochromatic Al Kα (1486.6 eV) source operated at 15 kV and 20 mA at a detection angle of 20° with respect to the sample normal. Binding energies are referred to the aliphatic C 1s emission at 285 eV. UPS spectra were acquired using a He I radiation source (21.2 eV) operated at 100 mA with normal detection at a constant pass energy of 2 eV.

Scanning Tunneling Microscopy. STM measurements were performed using a Scanning Probe Microscope AFM-STM 5500 (Agilent Technologies) isolated from vibrations, air turbulence, and acoustic noise. STM imaging was performed in a $HClO_4$ 0.1 M aqueous solution under electrochemical control using a four-electrode bipotentiostat for the independent control of substrate and tip potentials with respect to a reference electrode. A custom-made three-electrode PTFE cell was used with two Pt wires used as counter and pseudo-reference electrodes, respectively. Typical images were acquired in constant current mode under electrochemical bias using the following conditions. Au(111): 0.9 nA sample current, 300 mV sample bias, and 450 mV (vs SCE) sample potential; SAM modified surface: 0.7 nA sample current, 340 mV sample bias, and 350 mV (vs SCE) sample potential; PPIX deposited over SAM modified Au(111): 1.5 nA, 220 mV sample bias, and 250 mV (vs SCE) sample potential. W tips were made by etching in 2 M KOH and then cleaning with concentrated hydrofluoric acid, water, and acetone. To minimize Faradaic currents, the tips were isolated with nail paint and dried overnight. Tips were tested and calibrated imaging clean HOPG substrates obtaining atomically resolved images.

Near-Edge X-ray Absorption Fine Structure Spectroscopy. NEXAFS measurements were carried out at the Brazilian Synchrotron Light Source (LNLS), Campinas, Brazil, using the planar grating monochromator (PGM) beamline for soft X-ray spectroscopy (100−1500 eV) as the monochromatic photon source. Experiments were performed using the photoemission end station with a base pressure of 10^{-10} mbar. NEXAFS spectra were obtained by measuring the total electron yield (electron current at the sample) simultaneously with a photon flux monitor (electron current at a Au mesh). The final data were normalized with respect to the Au mesh electron current to correct for fluctuations in the beam intensity. NEXAFS spectra were recorded at normal 90° and at 35° photon incidence angle with respect to the sample surface. Note that it was not possible to measure at lower incidence angles due to geometric constrains. All angle dependent geometry effects (for example, sampling a different number of surface species) are eliminated by normalizing the resonant intensities to the angle-independent K-edge jump in all spectra.[22] The monochromator and thus the NEXAFS energy scale were not calibrated.

Surface-Enhanced Resonance Raman. SERR spectra were acquired employing a confocal microscope (Olympus BX40) coupled to a single-stage spectrograph (Dilor XY; f = 800 mm) equipped with a 1800 lines/mm grating and a liquid

DOI: 10.1021/acs.jpcc.7b04983
J. Phys. Chem. C XXXX, XXX, XXX−XXX

nitrogen-cooled back-illuminated CCD detector (2048 × 512 pixels). The 413 nm line of a continuous wave krypton ion laser (~3 mW; Spectra Physics BeamLok 2060) or the 514.5 nm line of a continuous wave argon ion laser (~12 mW; Coherent Innova 70C) was focused on a silver nanostructured surface by means of a long working distance objective (20×, NA 0.35), and the elastic scattering was rejected with Notch filters. The spectral accumulation times were between 5 and 10 s for 413 nm excitation and 20 s for 514 nm excitation. Before each experiment, the spectrometer was calibrated employing Hg and Ne calibration lamps (Newport), and all the spectra were obtained simultaneously with the 435.833 nm line from the Hg calibration lamp as an internal spectroscopic standard to ensure reproducibility. The spectrometer parameters were set to obtain a 0.4 cm^{-1} increment per data point and a 3 cm^{-1} instrumental bandpass. Ag disks employed for SERR measurements were treated by repetitive oxidation/reduction electrochemical cycles in 0.1 M KCl to create a SER-active nanostructured surface.

■ RESULTS AND DISCUSSION

PPIX molecules were covalently bonded to a self-assembled monolayer (SAM) of 16-amino-1-hexadecanethiol (NH_2C_{16}) on Au(111) surfaces via a carbodiimide-mediated amidation.[23] This method involves first growing the NH_2C_{16} SAM on the bare Au(111) surface. This is followed by the formation of an amide chemical bond between the −COOH chemical groups in the PPIX molecule and the $-NH_2$ functions in the SAM in aqueous solutions as shown in Scheme 1. Although the method has been used successfully to attach transition metal complexes to self-assembled monolayers on Au(111) surfaces,[24,25] in the present case, the reaction was very inefficient due to the low solubility of PPIX in water. Thus, different binary dimethyl sulfoxide:H_2O solutions were employed to carry out the reaction, with a 1:1 ratio giving reasonable yields.

Figure 1 shows the N 1s, C 1s, S 2p, and Au 4f XPS spectra corresponding to three different stages in the functionalization of the surface: (i) the initial Au(111) surface (black), (ii) after 16-amino-1-hexadecanethiol SAM formation (blue), and (iii) after PPIX attachment to the NH_2C_{16} SAM (red). The N 1s region also shows the reference spectrum corresponding to PPIX multilayers deposited over the Au(111) surface in the absence of the SAM (green). The initial surface shows only Au related signals in the XPS scans (see the Supporting Information). The absence of C, N, and S is to be noted, confirming that the substrate is atomically clean before growth of the molecular layers.

Formation of the NH_2C_{16} SAM results in the expected appearance of C, N, and S and in the attenuation of the Au 4f signal. The N 1s spectrum corresponding to the NH_2C_{16} SAM shows a broad signal with major contributions at ~400 eV due to the $-NH_2$ group and at ~402 eV due to the protonated amine $-NH_3^+$.[26] Note that a fraction of the amine terminal groups is expected to protonate in the acid−base equilibrium that takes place while rinsing. The C 1s signal shows a main peak centered at ~285 eV attributed to the hydrocarbon backbone of the $NH_2C_{16}SH$ molecules, whereas the S 2p region shows the characteristic doublet with the S $2p_{3/2}$ at ~162 eV, indicating the formation of a thiolate S−Au bond. The nominal N:C:S ratio is 1:16:1 and the XPS N:C:S ratio is 1:12:0.5, showing the attenuation in the S and C signals due to the overlaying atoms in the molecule and thus suggesting that the molecules adopt the expected orientation with the $-NH_2$ groups at the vacuum/monolayer interface. Three spectral

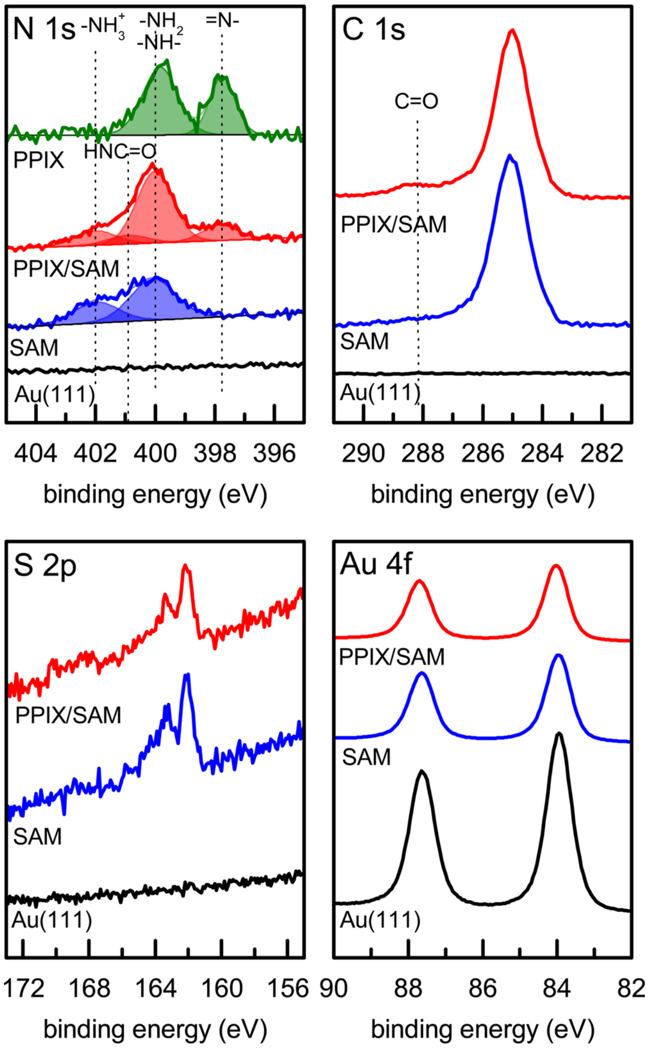

Figure 1. XPS spectra corresponding to the initial Au(111) surface (black), amine terminated self-assembled monolayers on Au(111) (blue), and PPIX attached to the SAM functionalized surface (red). N 1s, C 1s, S 2p, and Au 4f regions are displayed. The top spectrum in the N 1s region corresponds to PPIX multilayers deposited over Au(111) (green).

changes are observed when the PPIX molecules are bonded to the NH_2C_{16} SAM. First, the N 1s spectrum shows a new contribution at ~397.7 eV due to the two iminic ═N− atoms in the porphyrin molecules.[27] Note that the contribution of the two aminic −NH− atoms in the porphyrins is expected at ~400 eV (see multilayer spectrum) overlapping with the $-NH_2$ signal from the underlying SAM. The iminic and aminic signals are clearly seen in the spectrum corresponding to the deposition of PPIX multilayers (measured in the absence of the SAM). Furthermore, there is a small contribution at ~400.8 eV due to the amide bond −NC═O[28] formed once the molecules are attached to the SAM. The amide:iminic integrated intensity ratio is 1:2, suggesting that the molecules are anchored to the SAM via one amide bond. Second, the C 1s spectrum presents an small feature at ~288.2 eV which could be attributed to carbonyl carbons[29] in the carboxy and amide functional groups and tentatively to a shakeup satellite present in organic molecules with extended conjugated π systems. Finally, the Au 4f signal is further attenuated as the film thickness increases after binding PPIX molecules to the

DOI: 10.1021/acs.jpcc.7b04983
J. Phys. Chem. C XXXX, XXX, XXX−XXX

NH_2C_{16} SAM. Given that the expected surface coverage of NH_2C_{16} SAMs over Au(111) is ~$4{\cdot}10^{14}$ molecules cm^{-2},[30] and that the SAM:PPIX ratio calculated from the N 1s XPS signals is 1:0.09, then the estimated PPIX surface coverage is ~$3.6{\cdot}10^{13}$ molecules cm^{-2}, in line with the value estimated from the UV–vis measurements discussed in the Supporting Information.

Figure 2 shows the UPS spectra of NH_2C_{16} SAM/Au(111) (blue) and PPIX/SAM/Au(111) (red) in comparison to the spectrum of the clean Au(111) surface (black). The left panel shows the secondary electron cutoff, and the right panel shows the region around the Fermi edge. The UPS spectrum corresponding to the bare Au(111) substrate is very similar to that previously reported.[31] From its width, we can calculate the Au(111) work function (Φ):[32] Φ = 21.21 eV − W = 5.35 eV, which is in excellent agreement with values reported elsewhere.[33] Formation of the NH_2C_{16} SAM over the Au(111) surface shifted the position of the secondary electron cutoff, resulting in a work function change (ΔΦ) of approximately −1.84 eV (within the experimental uncertainty of 0.05 eV). This value is in agreement with the values reported for similar systems and implies that the chemisorbed alkanethiols form a dipole layer with negative charges residing at the metal/monolayer interface and positive charges at the monolayer/vacuum interface.[34] Incorporation of PPIX molecules on the monolayer modifies the work function only slightly (ΔΦ = −1.56 eV), implying that the surface dipole layer is still dominated by the NH_2C_{16} SAM. The right panel of Figure 2 shows that formation of the NH_2C_{16} SAM results in a complete attenuation of the 5d and broad 6s Au bands with no discernible new contributions to the electronic density in the region below the Fermi edge. Bonding of PPIX molecules to the SAM resulted in a very small, yet discernible, peak at −1.95 eV below the Fermi edge which can be easily seen after subtracting the SAM spectrum (shown in the inset). This new electronic state can be tentatively assigned to the HOMO state in the PPIX molecules.[35]

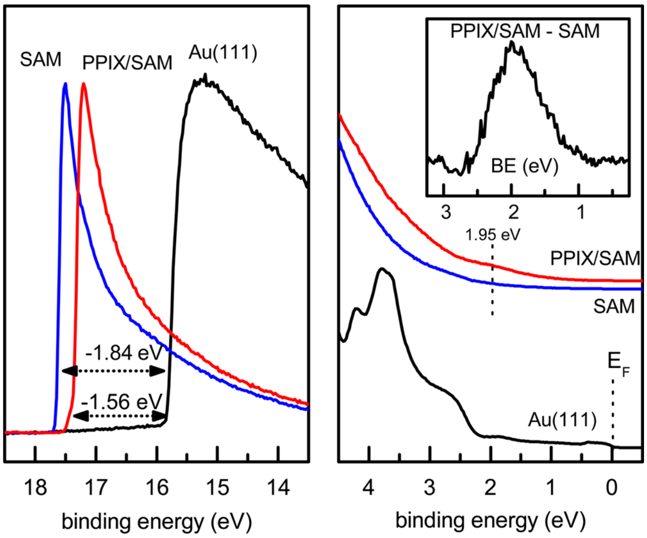

Figure 2. UPS spectra corresponding to the initial Au(111) surface (black), amine terminated self-assembled monolayers on Au(111) (blue), and PPIX attached to the SAM functionalized surface (red). Left panel shows the secondary electron cutoff, the right panel shows the region below the Fermi edge, and the inset shows the difference between the PPIX/SAM and the SAM spectra.

Figure 3 shows STM images corresponding to the initial Au(111) surface, after growth of the NH_2C_{16} SAM on Au(111) and after attachment of PPIX molecules to the SAM. Also shown are line profiles corresponding to each image. Large terraces separated by monatomic steps are observed in the images corresponding to the clean Au(111) surface. Deposition of the NH_2C_{16} SAM results in the appearance of dark areas corresponding to pits of monatomic depth which are induced by the dynamic self-assembly process that takes place during the formation of the monolayer in solution.[24,25] Covalent attachment of PPIX molecules to the NH_2C_{16} SAM results in randomly distributed bright spots with a broad size distribution.

The XPS, UPS, and STM results discussed above provide experimental evidence confirming the covalent attachment of

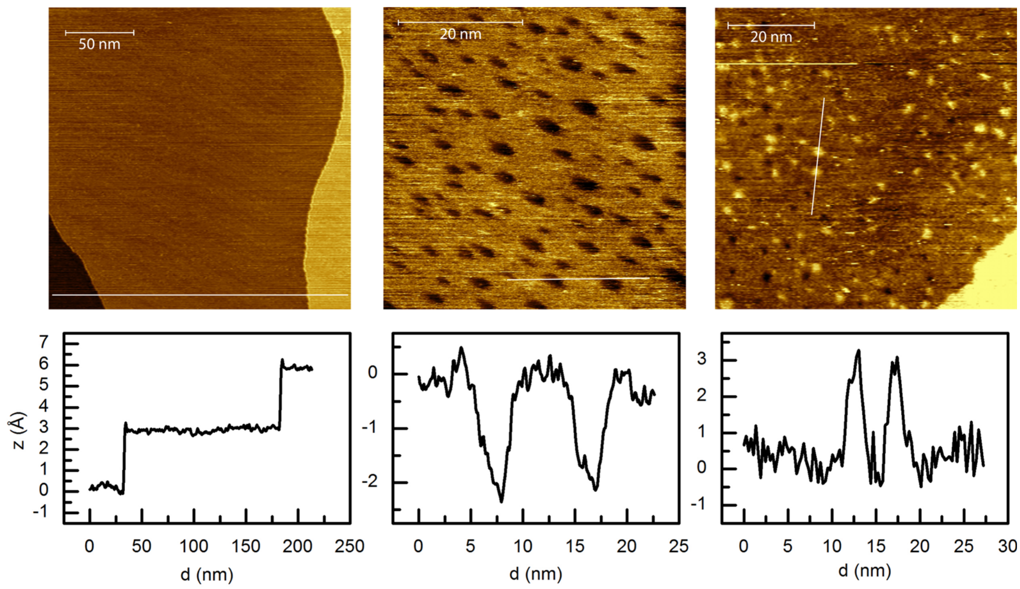

Figure 3. STM images corresponding to the initial Au(111) surface (left), amine terminated self-assembled monolayers on Au(111) (center), and PPIX attached to the SAM functionalized surface (right).

DOI: 10.1021/acs.jpcc.7b04983
J. Phys. Chem. C XXXX, XXX, XXX−XXX

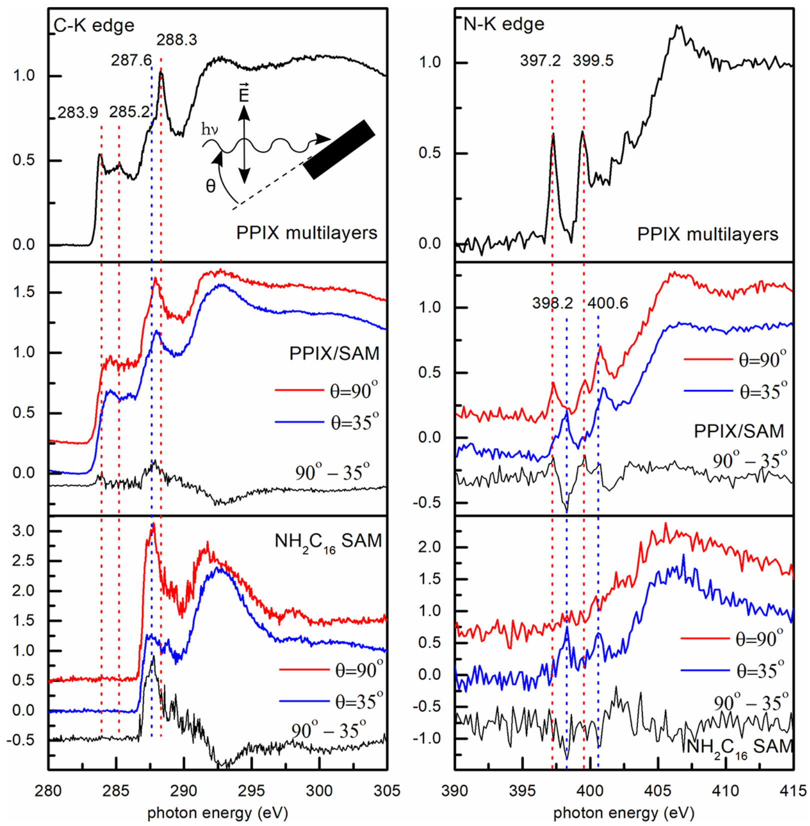

Figure 4. C edge and N edge normalized NEXAFS spectra of the amine terminated self-assembled monolayers on Au(111) (NH_2C_{16} SAM) and PPIX attached to the SAM functionalized surface (PPIX/SAM). The spectra were taken at incidence angles of 35° and 90°. Top graph shows the reference spectrum corresponding to PPIX multilayers.

PPIX molecules to the NH_2C_{16} SAM on Au(111). Additional evidence is provided by examining the C and N K-edge NEXAFS spectra shown in Figure 4. The angle resolved carbon edge spectra corresponding to the NH_2C_{16} SAM, to PPIX molecules attached to the SAM functionalized surface (PPIX/SAM), and to multilayers of PPIX directly deposited on the naked metal surface are shown on the left panel. The respective N edge spectra are shown on the right panel. The C edge NEXAFS spectra corresponding to the NH_2C_{16} SAM are dominated by a resonance at ∼287.6 eV which has been assigned to a transition from C 1s into C−H σ^*[36] and also to excitations into orbitals of dominantly Rydberg character.[37] The other prominent feature in the spectra is a broad resonance at ∼293 eV which is assigned to a transition from C 1s into C−C σ^*.[36] The relative intensities of these resonances change in opposite directions as the angle of incidence is modified. The C−H σ^* resonance (oriented perpendicular to the alkyl chains axis)[38] is strongest at normal incidence (i.e., when the electric field of the incoming radiation is parallel to the surface) and decreases when the incidence angle is reduced, whereas the C−C σ^* resonance (oriented along the chains axis)[38] exhibits the opposite behavior. This implies that the alkyl chain molecular axis in the self-assembled monolayer is in an upright configuration as expected.[30,36,39] Attaching PPIX molecules to the SAM results in the C 1s NEXAFS spectra shown in the left center panel of Figure 4. New resonance transitions appear below 286 eV in addition to the transitions due to the underlying SAM. Interpretation of these spectra requires using the spectrum corresponding to PPIX multilayers shown in the top panel. The C 1s NEXAFS spectra of PPIX/SAM could be arbitrarily divided in three regions: (i) the region between 283 and ∼286 eV where many C 1s → π^* transitions in the PPIX molecules are expected,[40] (ii) the region between ∼286 and ∼290 eV where Rydberg, C 1s → C−H σ^*, and other[40] transitions are expected, and finally (iii) the region above 290 eV dominated by C 1s → σ^* transitions. The first region is the only one presenting signals due to only the PPIX molecules as the SAM does not have π electronic density; in the other two regions, there is an overlap of signals from the SAM and PPIX molecules. The resonance at 283.9 eV can be assigned to a C 1s → π^* transition in the PPIX molecule.[41] For aromatic systems such as the porphine, the π^* states are derived from p_z orbitals oriented perpendicular to the molecular plane. If the aromatic π^* system lies normal to the surface, the C 1s → π^* transition intensity exhibits a maximum for $\theta = 90°$ and vanishes for $\theta = 0°$. Although the quality of the data is not good enough to estimate a tilt angle for the molecular plane, comparison of the 90° and 35° spectra shows that the intensity of the C 1s → π^* transition at 283.9 eV is slightly larger in the former case. Although the sign and amplitude of the anisotropy in the maximum of the 90° − 35° difference spectrum is extremely small, it nevertheless suggests that the PPIX molecules are not flat-lying over the SAM, in line with SERR measurements discussed below.

The N edge NEXAFS spectra shown on the right panel of Figure 4 are consistent with the respective C edge NEXAFS spectra discussed above. The spectra corresponding to the NH_2C_{16} SAM in the bottom panel display three resonances and are very similar to those measured elsewhere.[26] The resonances at 398.2 and 400.6 eV have been assigned to N 1s → N−H σ^*

DOI: 10.1021/acs.jpcc.7b04983
J. Phys. Chem. C XXXX, XXX, XXX−XXX

transitions in the protonated and unprotonated amine groups in the monolayer, respectively,[26] whereas the ∼406 eV resonance has been assigned to N 1s → C−N σ^*. In line with the previously studied system[26] and with the known orientation of the NH_2C_{16} molecules in the SAM, the intensities of the first two transitions decrease with increasing the photon incidence angle.[26] Attaching PPIX molecules to the SAM results in at least two extra signals: The first one at 397.2 eV which has been assigned to N 1s → π^* (=N−) transitions and the second one at 399.5 eV due to N 1s → π^* (−NH−) transitions.[42] These PPIX related signals can be clearly seen in the spectrum corresponding to the PPIX multilayers shown in the top panel. The intensity dependence of the PPIX signals with photon incidence angle can be inferred from the 90° − 35° difference spectrum. Again, the quality of the data is not good enough to estimate a tilt angle; however, both N 1s → π^* transitions have slightly larger intensities at normal incidence, suggesting that the PPIX molecules are not flat-lying over the SAM, in line with the C 1s NEXAFS measurements discussed above and the SERR measurements discussed below.

Attachment of PPIX molecules to the NH_2C_{16} SAM was also studied with surface enhanced resonance raman spectroscopy (SERR). Figure 5 shows SERR spectra (1100−1700 cm^{-1}) corresponding to PPIX molecules bonded to NH_2C_{16} SAM over nanostructured Ag. Also shown is the spectrum corresponding to PPIX multilayers and, in the top panel, the PPIX/SAM spectrum measured with 514 nm excitation laser. SERR measurements were conducted using nanostructured Ag instead of Au(111) substrates in order to attain simultaneous resonance with the electronic transitions of the porphyrin and with the surface plasmons of the metal substrate, thus obtaining maximal signal enhancement.[43] Using Ag instead of Au for the SERR measurements should not influence PPIX bonding to the NH_2C_{16} SAM because: (i) long alkylthiol chains are employed in the SAM detaching a possible influence from the substrate and (ii) amine terminated alkylthiol SAMs are known to form compact monolayers similar to those formed over Au substrates.[44] The observed bands correspond to the PPIX molecules as the underlying SAM has no significant contribution under the experimental conditions employed. Band assignment[45] is indicated by the labeling of SERR bands shown in Figure 5 and confirms that the molecules bind to the surface, retaining their molecular integrity. The top panel of Figure 5 shows the PPIX/SAM SERR spectrum obtained under Q-band excitation (514 nm). Under these conditions, SERR spectra are weaker, but sensitive, to the orientation of the molecular plane relative to the surface.[46] In an ideal D_{4h} porphyrin symmetry, the A_{1g} modes will experience preferential enhancement when the molecular plane is parallel to the surface, whereas the B_{1g} mode will be enhanced for a perpendicular orientation. Therefore, the $\nu_{10}(B_{1g})$:$\nu_4(A_{1g})$ intensity ratio is indicative of the molecular orientation.[46] The Q-band excited spectrum of the PPIX molecules bonded to the NH_2C_{16} SAM shows that the intensity of the $\nu_{10}(B_{1g})$ band is greater than the intensity of the $\nu_4(A_{1g})$ band, indicating an adsorption geometry where the molecular plane is not flat-lying, in agreement with the NEXAFS results discussed above.

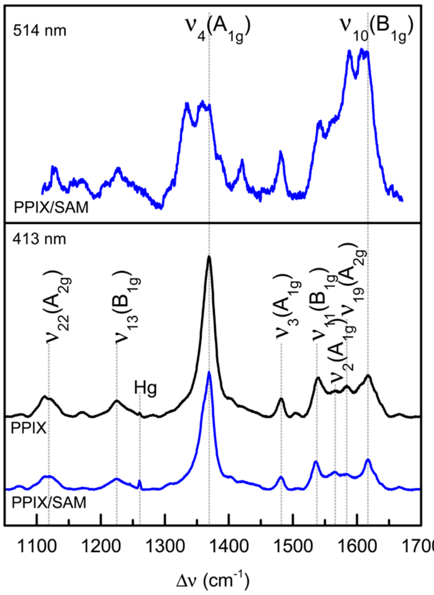

Figure 5. SERR spectra of PPIX molecules attached to the NH_2C_{16} SAM (PPIX/SAM). Also shown is the spectrum of PPIX multilayers (PPIX). Spectra were measured under Soret (413 nm) excitation, whereas the top spectrum was measured under Q-band (514 nm) excitation.

The data discussed above demonstrate that the PPIX molecules are covalently bonded to the NH_2C_{16} SAM and that the molecular plane is tilted. This system can be employed to study the insertion of cations from solution into the center of the porphyrin ring. Figure 6 shows the N 1s and Zn $2p_{3/2}$ XPS spectra (red) before and after exposing the PPIX/SAM/Au(111) surface to a 0.01 M Zn^{2+} solution at room temperature for 1 h. Figure 6 also shows the spectra (blue) before and after exposing the NH_2C_{16} SAM/Au(111) to the Zn^{2+} solution. Exposing the SAM to Zn^{2+} does not result in any significant change in the N 1s spectrum. Furthermore, the absence of Zn^{2+} on the surface indicates that rinsing removes all cations that could be interacting with the amine groups when the SAM was in contact with the solution. However, exposing the PPIX/SAM/Au(111) surface to Zn^{2+} results in the presence of Zn on the surface even after extensive rinsing. The amount of Zn left on the surface corresponds to metalation of 20% of

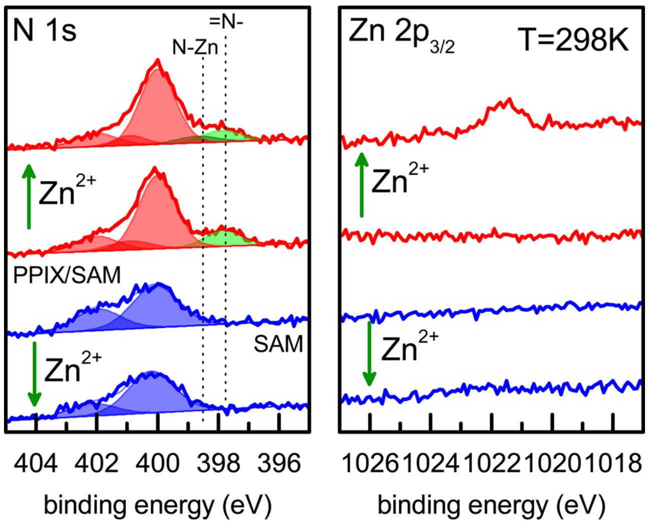

Figure 6. N 1s and Zn $2p_{3/2}$ XPS spectra of NH_2C_{16} SAM molecules (blue) and of PPIX molecules attached to the NH_2C_{16} SAM (red) before and after exposing the surface to a 0.01 M Zn^{2+} aqueous solution at room temperature.

DOI: 10.1021/acs.jpcc.7b04983
J. Phys. Chem. C XXXX, XXX, XXX−XXX

the PPIX molecules attached to the SAM. Indeed, the N 1s spectrum measured after placing the system in contact with the Zn^{2+} solution could be fitted with a new component at ∼398.5 eV that corresponds to the metalated porphyrin molecules (N-Zn) (see Figure 7) and has an integrated intensity

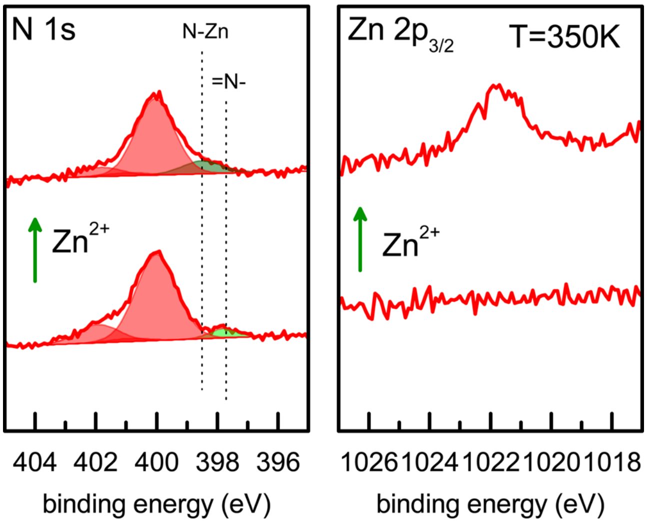

Figure 7. N 1s and Zn $2p_{3/2}$ XPS spectra of PPIX molecules attached to the NH_2C_{16} SAM before and after exposing the surface to a 0.01 M Zn^{2+} aqueous solution at 350 K.

corresponding to a metalation of 20%. These results are in line with the solution behavior of porphyrin molecules. Indeed, metalation of similar porphyrin molecules with Zn^{2+} in protic solvents at room temperature has a half-life between 2 and 6 h.[47] Thus, increasing the reaction temperature should result in a larger extent of metalation as shown below.

Figure 7 shows the N 1s and Zn $2p_{3/2}$ XPS spectra before and after exposing the PPIX/SAM/Au(111) surface to a 0.01 M Zn^{2+} solution at 350 K for 1 h. Exposing the molecules to Zn^{2+} at 350 K results in the absence of the 397.7 eV component corresponding to the iminic nitrogens and the appearance of a new component at 398.5 eV due to the equivalent nitrogen atoms in the metalated molecules. Furthermore, the amount of Zn measured on the surface corresponds to complete metalation, thus indicating that the molecules are fully metalated at 350 K.

Metalation with Zn^{2+} at the solid−liquid interface was also studied for a monolayer of PPIX molecules adsorbed directly on Au(111). Figure 8 shows the N 1s and Zn $2p_{3/2}$ XPS spectra before and after exposing the PPIX/Au(111) surface to a 0.01 M Zn^{2+} solution at room temperature for 1 h. The surface coverage of PPIX molecules directly adsorbed on Au(111) is close to a monolayer, and the molecules are expected to be interacting with the surface in a flat-lying geometry.[48] The PPIX spectrum of the monolayer before exposure to the solution exhibits the two distinct N 1s peaks expected for the two aminic and two iminic nitrogen atoms as discussed above. After exposure to 0.01 M Zn^{2+} solution for 1 h, only one peak is observed at 398.5 eV with the combined area of the two nitrogen peaks of the monolayer before exposure to the solution. The change is accompanied by a Zn $2p_{3/2}$ signal at 1021.6 eV with a nitrogen-to-zinc ratio of 3.8:1 (when corrected for sensitivity factors), very close to the expected ratio of 4:1 for ZnPPIX, thus, indicating full metalation of PPIX molecules adsorbed on Au(111) at room temperature, in

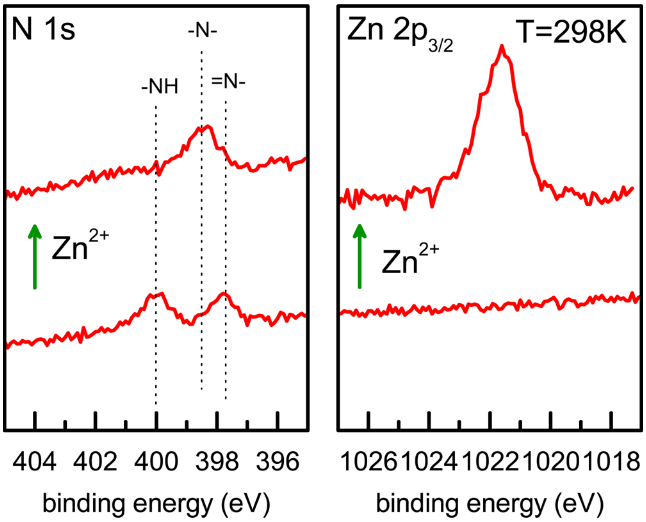

Figure 8. N 1s and Zn $2p_{3/2}$ XPS spectra of PPIX molecules deposited directly over Au(111) before and after exposing the surface to a 0.01 M Zn^{2+} aqueous solution at room temperature.

agreement with the behavior of 2HTPP monolayers.[19] The results discussed above suggest that the reaction pathway followed for the metalation of PPIX molecules adsorbed on Au(111) has a lower activation barrier than the pathway followed when the molecules are bonded to the SAM. This is in line with the observed distortion of the macrocycle center after adsorption on metal surfaces[49] which could tentatively lower the activation barrier for the insertion of the cation.

■ CONCLUSIONS

Porphyrin molecules functionalized with carboxylic acid groups can be covalently bonded to an amine terminated alkanethiol self-assembled monolayer on Au(111) via a carbodiimide-mediated amidation. The porphyrin molecules maintain their molecular and electronic structure after surface attachment. The molecular layer generates a surface dipole that decreases the metal work function, and the HOMO molecular orbital is situated ∼2 eV below the Au(111) Fermi edge. NEXAFS and SERR measurements indicate that the molecules are bonded with a tilted molecular plane. XPS experiments show that full metalation of PPIX molecules bonded to the SAM with Zn^{2+} cations requires higher temperatures than metalation when PPIX molecules interact directly with the Au(111) surface. This finding suggests that the molecule−substrate interaction could lower the reaction activation barrier.

■ ASSOCIATED CONTENT

Supporting Information

The Supporting Information is available free of charge on the ACS Publications website at DOI: 10.1021/acs.jpcc.7b04983.

XPS spectrum of the bare Au(111) surface (Figure S1). UV−vis absorption spectrum of PPIX molecules attached to the SAM over semitransparent Au (Figure S2). Estimation of the surface coverage of PPIX molecules attached to the SAM from the Soret band absorption intensity (Figure S3) (PDF)

DOI: 10.1021/acs.jpcc.7b04983
J. Phys. Chem. C XXXX, XXX, XXX−XXX

AUTHOR INFORMATION

Corresponding Author

*E-mail: fwilliams@qi.fcen.uba.ar. Phone: +54 11 45763380. Fax: +54 11 45763341.

ORCID

Daniel H. Murgida: 0000-0001-5173-0183

Federico J. Williams: 0000-0002-6194-2734

Notes

The authors declare no competing financial interest.

ACKNOWLEDGMENTS

Funding from CONICET and AGENCIA is graciously acknowledged. Part of the research was undertaken in the PGM beamline of the Brazilian Synchrotron Light Laboratory LNLS. We acknowledge LNLS for financial support to use their facilities.

REFERENCES

(1) Milgrom, L. R. *The Colours of Life: An Introduction to the Chemistry of Porphyrins and Related Compounds*; Oxford University Press: Oxford, U.K., 1997.

(2) Gao, W.-Y.; Chrzanowski, M.; Ma, S. Metal-Metalloporphyrin Frameworks: A Resurging Class of Functional Materials. *Chem. Soc. Rev.* **2014**, *43*, 5841−5866.

(3) Forrest, S. R.; Baldo, M. A.; O'Brien, D. F.; You, Y.; Shoustikov, A.; Sibley, S.; Thompson, M. E. Highly Efficient Phosphorescent Emission from Organic Electroluminescent Devices. *Nature* **1998**, *395*, 151−154.

(4) Yella, A.; Lee, H.-W.; Tsao, H. N.; Yi, C.; Chandiran, A. K.; Nazeeruddin, M. K.; Diau, E. W.-G.; Yeh, C.-Y.; Zakeeruddin, S. M.; Gratzel, M. Porphyrin-Sensitized Solar Cells with Cobalt (II/III)-Based Redox Electrolyte Exceed 12% Efficiency. *Science* **2011**, *334*, 629−634.

(5) Costentin, C.; Dridi, H.; Savéant, J.-M. Molecular Catalysis of O_2 Reduction by Iron Porphyrins in Water: Heterogeneous versus Homogeneous Pathways. *J. Am. Chem. Soc.* **2015**, *137*, 13535−13544.

(6) Jurow, M.; Schuckman, A. E.; Batteas, J. D.; Drain, C. M. Porphyrins as Molecular Electronic Components of Functional Devices. *Coord. Chem. Rev.* **2010**, *254*, 2297−2310.

(7) Imahori, H.; Fukuzumi, S. Porphyrin- and Fullerene-Based Molecular Photovoltaic Devices. *Adv. Funct. Mater.* **2004**, *14*, 525−536.

(8) Ding, Y.; Zhu, W.-H.; Xie, Y. Development of Ion Chemosensors Based on Porphyrin Analogues. *Chem. Rev.* **2017**, *117*, 2203−2256.

(9) Fenwick, O.; Sprafke, J. K.; Binas, J.; Kondratuk, D. V.; Di Stasio, F.; Anderson, H. L.; Cacialli, F. Linear and Cyclic Porphyrin Hexamers as Near-Infrared Emitters in Organic Light-Emitting Diodes. *Nano Lett.* **2011**, *11*, 2451−2456.

(10) Vaughan, O. P. H.; Williams, F. J.; Bampos, N.; Lambert, R. M. A Chemically Switchable Molecular Pinwheel. *Angew. Chem., Int. Ed.* **2006**, *45*, 3779−3781.

(11) Gottfried, J. M. Surface Chemistry of Porphyrins and Phthalocyanines. *Surf. Sci. Rep.* **2015**, *70*, 259−379.

(12) Auwärter, W.; Écija, D.; Klappenberger, F.; Barth, J. V. Porphyrins at Interfaces. *Nat. Chem.* **2015**, *7*, 105−120.

(13) Cotton, T. M.; Schultz, S. G.; Van Duyne, R. P. Surface-Enhanced Resonance Raman Scattering from Water-Soluble Porphyrins Adsorbed on a Silver Electrode. *J. Am. Chem. Soc.* **1982**, *104*, 6528−6532.

(14) Auwärter, W.; Weber-Bargioni, A.; Brink, S.; Riemann, A.; Schiffrin, A.; Ruben, M.; Barth, J. V. Controlled Metalation of Self-Assembled Porphyrin Nanoarrays in Two Dimensions. *ChemPhysChem* **2007**, *8*, 250−254.

(15) Diller, K.; Papageorgiou, A. C.; Klappenberger, F.; Allegretti, F.; Barth, J. V.; Auwärter, W. In Vacuo Interfacial Tetrapyrrole Metallation. *Chem. Soc. Rev.* **2016**, *45*, 1629−1656.

(16) Di Santo, G.; Castellarin-Cudia, C.; Fanetti, M.; Taleatu, B.; Borghetti, P.; Sangaletti, L.; Floreano, L.; Magnano, E.; Bondino, F.; Goldoni, A. Conformational Adaptation and Electronic Structure of 2H-Tetraphenylporphyrin on Ag(111) during Fe Metalation. *J. Phys. Chem. C* **2011**, *115*, 4155−4162.

(17) Diller, K.; Klappenberger, F.; Marschall, M.; Hermann, K.; Nefedov, A.; Wöll, C.; Barth, J. V. Self-Metalation of 2H-Tetraphenylporphyrin on Cu(111): An X-Ray Spectroscopy Study. *J. Chem. Phys.* **2012**, *136*, 014705.

(18) Schneider, J.; Franke, M.; Gurrath, M.; Röckert, M.; Berger, T.; Bernardi, J.; Meyer, B.; Steinrück, H.-P.; Lytken, O.; Diwald, O. Porphyrin Metalation at MgO Surfaces: A Spectroscopic and Quantum Mechanical Study on Complementary Model Systems. *Chem. - Eur. J.* **2016**, *22*, 1744−1749.

(19) Franke, M.; Marchini, F.; Steinrück, H.-P.; Lytken, O.; Williams, F. J. Surface Porphyrins Metalate with Zn Ions from Solution. *J. Phys. Chem. Lett.* **2015**, *6*, 4845−4849.

(20) Franke, M.; Marchini, F.; Jux, N.; Steinrück, H.-P.; Lytken, O.; Williams, F. J. Zinc Porphyrin Metal-Center Exchange at the Solid-Liquid Interface. *Chem. - Eur. J.* **2016**, *22*, 8520−8524.

(21) Méndez De Leo, L. P.; de la Llave, E.; Scherlis, D.; Williams, F. J. Molecular and Electronic Structure of Electroactive Self-Assembled Monolayers. *J. Chem. Phys.* **2013**, *138*, 114707.

(22) Stöhr, J.; Outka, D. A. Determination of Molecular Orientations on Surfaces from the Angular Dependence of Near-Edge X-Ray-Absorption Fine-Structure Spectra. *Phys. Rev. B: Condens. Matter Mater. Phys.* **1987**, *36*, 7891−7905.

(23) Shegal, D.; Vijay, I. A Method for the High Efficiency of Water-soluble Carbodiimide-Mediated Amidation. *Anal. Biochem.* **1994**, *218*, 87−91.

(24) de la Llave, E.; Herrera, S. E.; Méndez De Leo, L. P.; Williams, F. J. Molecular and Electronic Structure of Self-Assembled Monolayers Containing Ruthenium(II) Complexes on Gold Surfaces. *J. Phys. Chem. C* **2014**, *118*, 21420−21427.

(25) de la Llave, E.; Herrera, S. E.; Adam, C.; Méndez De Leo, L. P.; Calvo, E. J.; Williams, F. J. Molecular and Electronic Structure of Osmium Complexes Confined to Au(111) Surfaces Using a Self-Assembled Molecular Bridge. *J. Chem. Phys.* **2015**, *143*, 184703.

(26) Baio, J.; Weidner, T.; Brison, J.; Graham, D.; Gamble, L. J.; Castner, D. G. Amine Terminated SAMs: Investigating why Oxygen is Present in These Films. *J. Electron Spectrosc. Relat. Phenom.* **2009**, *172*, 2−8.

(27) Karweik, D. H.; Winograd, N. Nitrogen Charge Distributions in Free-Base Porphyrins, Metalloporphyrins, and Their Reduced Analogs Observed by X-Ray Photoelectron Spectroscopy. *Inorg. Chem.* **1976**, *15*, 2336−2342.

(28) Graf, N.; Yegen, E.; Gross, T.; Lippitz, A.; Weigel, W.; Krakert, S.; Terfort, A.; Unger, W. E. XPS and NEXAFS Studies of Aliphatic and Aromatic Amine Species on Functionalized Surfaces. *Surf. Sci.* **2009**, *603*, 2849−2860.

(29) Saavedra, H. M.; Thompson, C. M.; Hohman, J. N.; Crespi, V. H.; Weiss, P. S. Reversible Lability by in Situ Reaction of Self-Assembled Monolayers. *J. Am. Chem. Soc.* **2009**, *131*, 2252−2259.

(30) Strong, L.; Whitesides, G. M. Structures of Self-Assembled Monolayer Films of Organosulfur Compounds Adsorbed on Gold Single Crystals: Electron Diffraction Studies. *Langmuir* **1988**, *4*, 546−558.

(31) Rieley, H.; Price, N.; White, R.; Blyth, R.; Robinson, a. W. A NEXAFS and UPS Study of Thiol Monolayers Self-Assembled on Gold. *Surf. Sci.* **1995**, *331−333*, 189−195.

(32) Torasso, N.; Armaleo, J. M.; Tagliazucchi, M.; Williams, F. J. Simplified Approach to Work Function Modulation in Polyelectrolyte Multilayers. *Langmuir* **2017**, *33*, 2169−2176.

(33) De Renzi, V.; Rousseau, R.; Marchetto, D.; Biagi, R.; Scandolo, S.; del Pennino, U. Metal Work-Function Changes Induced by Organic Adsorbates: A Combined Experimental and Theoretical Study. *Phys. Rev. Lett.* **2005**, *95*, 046804.

(34) Alloway, D. M.; Hofmann, M.; Smith, D. L.; Gruhn, N. E.; Graham, A. L.; Colorado, R., Jr.; Wysocki, V. H.; Lee, T. R.; Lee, P. A.;

DOI: 10.1021/acs.jpcc.7b04983
J. Phys. Chem. C XXXX, XXX, XXX−XXX

Armstrong, N. R. Interface Dipoles Arising from Self-Assembled Monolayers on Gold: UV - Photoemission Studies of Alkanethiols and Partially Fluorinated Alkanethiols. *J. Phys. Chem. B* **2003**, *107*, 11690−11699.

(35) Papageorgiou, A. C.; Fischer, S.; Oh, S. C.; Saglam, Ö.; Reichert, J.; Wiengarten, A.; Seufert, K.; Vijayaraghavan, S.; Écija, D.; Auwärter, W.; et al. Self-Terminating Protocol for an Interfacial Complexation Reaction in Vacuo by Metal-Organic Chemical Vapor Deposition. *ACS Nano* **2013**, *7*, 4520−4526.

(36) Hähner, G.; Kinzler, M.; Wöll, C.; Grunze, M.; Scheller, M. K.; Cederbaum, L. S. Near Edge X-Ray-Absorption Fine-Structure Determination of Alkyl-Chain Orientation: Breakdown of the "Building-Block" Scheme. *Phys. Rev. Lett.* **1991**, *67*, 851−854.

(37) Bagus, P.; Weiss, K.; Schertel, A.; Wöll, C.; Braun, W.; Hellwig, C.; Jung, C. Identification of Transitions into Rydberg States in the X-Ray Absorption Spectra of Condensed Long-Chain Alkanes. *Chem. Phys. Lett.* **1996**, *248*, 129−135.

(38) Frey, S.; Heister, K.; Zharnikov, M.; Grunze, M. Modification of Semifluorinated Alkanethiolate Monolayers by Low Energy Electron Irradiation. *Phys. Chem. Chem. Phys.* **2000**, *2*, 1979−1987.

(39) Himmel, H.-J.; Weiss, K.; Jäger, B.; Dannenberger, O.; Grunze, M.; Wöll, C. Ultrahigh Vacuum Study on the Reactivity of Organic Surfaces Terminated by OH and COOH Groups Prepared by Self-Assembly of Functionalized Alkanethiols on Au Substrates. *Langmuir* **1997**, *13*, 4943−4947.

(40) Schmidt, N.; Fink, R.; Hieringer, W. Assignment of Near-Edge X-Ray Absorption Fine Structure Spectra of Metalloporphyrins by Means of Time-Dependent Density-Functional Calculations. *J. Chem. Phys.* **2010**, *133*, 054703.

(41) Diller, K.; Klappenberger, F.; Allegretti, F.; Papageorgiou, A. C.; Fischer, S.; Duncan, D. A.; Maurer, R. J.; Lloyd, J. A.; Oh, S. C.; Reuter, K.; et al. Temperature-Dependent Templated Growth of Porphine Thin Films on the (111) Facets of Copper and Silver. *J. Chem. Phys.* **2014**, *141*, 144703.

(42) Polzonetti, G.; Carravetta, V.; Iucci, G.; Ferri, A.; Paolucci, G.; Goldoni, A.; Parent, P.; Laffon, C.; Russo, M. Electronic Structure of Platinum Complex/Zn-Porphyrinato Assembled Macrosystems, Related Precursors and Model Molecules, as Probed by X-Ray-Absorption Spectroscopy (NEXAFS): Theory and Experiment. *Chem. Phys.* **2004**, *296*, 87−100.

(43) Todorovic, S.; Murgida, D. H. *Encyclopedia of Analytical Chemistry*; John Wiley & Sons, Ltd.: Chichester, U.K., 2016; pp 1−29.

(44) Marmisollé, W. A.; Capdevila, D. A.; de la Llave, E.; Williams, F. J.; Murgida, D. H. Self-Assembled Monolayers of NH_2-Terminated Thiolates: Order, pKa and Specific Adsorption. *Langmuir* **2013**, *29*, 5351−5359.

(45) Kitagawa, T.; Abe, M.; Ogoshi, H. Resonance Raman spectra of Octaethylporphyrinato-Ni(II) and Meso-Deuterated and 15 N Substituted Derivatives. I. Observation and Assignments of Nonfundamental Raman Lines. *J. Chem. Phys.* **1978**, *69*, 4516−4525.

(46) Kranich, A.; Ly, H. K.; Hildebrandt, P.; Murgida, D. H. Direct Observation of the Gating Step in Protein Electron Transfer: Electric-Field-Controlled Protein Dynamics. *J. Am. Chem. Soc.* **2008**, *130*, 9844−9848.

(47) Orzeł, Ł.; Kania, A.; Rutkowska-Zbik, D.; Susz, A.; Stochel, G.; Fiedor, L. Structural and Electronic Effects in the Metalation of Porphyrinoids. Theory and Experiment. *Inorg. Chem.* **2010**, *49*, 7362−7371.

(48) González-Moreno, R.; Sánchez-Sánchez, C.; Trelka, M.; Otero, R.; Cossaro, A.; Verdini, A.; Floreano, L.; Ruiz-Bermejo, M.; García-Lekue, A.; Martín-Gago, J. A.; et al. Following the Metalation Process of Protoporphyrin IX with Metal Substrate Atoms at Room Temperature. *J. Phys. Chem. C* **2011**, *115*, 6849−6854.

(49) Lepper, M.; Köbl, J.; Schmitt, T.; Gurrath, M.; de Siervo, A.; Schneider, M. A.; Steinrück, H.-P.; Meyer, B.; Marbach, H.; Hieringer, W. "Inverted" Porphyrins: A Distorted Adsorption Geometry of Free-Base Porphyrins on Cu(111). *Chem. Commun.* **2017**, *53*, 8207−8210.

DOI: 10.1021/acs.jpcc.7b04983
J. Phys. Chem. C XXXX, XXX, XXX−XXX